Contract No.:

This manuscript has been authored by Battelle Savannah River Alliance (BSRA), LLC under Contract No. 89303321CEM000080 with the U.S. Department of Energy (DOE) Office of Environmental Management (EM).

Investigating the effects Ag, Cu, and Pd functionalized chabazite have on the adsorption affinities of the noble gases Xe, Kr, and Ar.

M. A. Torcivia*[a], Steven M. E. Demers [a], Katherine L. Broadwater [a], Douglas B. Hunter [a]

a. Savannah River National Laboratory, P. O. Box A, Aiken, SC 29808, USA

*michael.torcivia@srnl.doe.gov, Phone: 803-646-2684

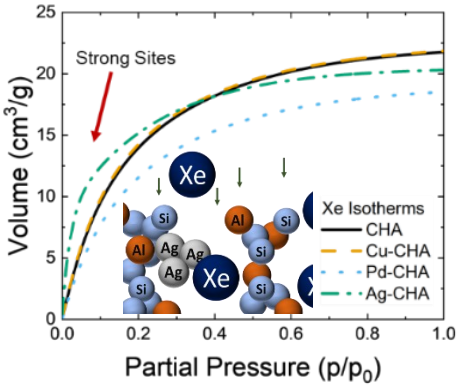

TOC Graphic

Abstract

Separation of the noble gases from air is typically done through a cryogenic distillation process that is both energy intensive and expensive. Ag functionalized zeolites and MOFs have a well-documented affinity for Xe and, to a lesser extent, Kr that could serve as more economic alternatives to this process on a commercial scale. The mechanism driving the Ag-Xe interaction, however, is still a matter of debate, and the use of other metals in place of Ag is not as thoroughly documented. In this study, Ag, Cu, and Pd functionalized chabazite specimens were prepared, and their affinities for the noble gases Xe, Kr, and Ar were investigated and compared to each other and an unexchanged Na-chabazite. From these analyses, Ag functionalized chabazite displayed the highest affinity for Xe among these samples, but there was not a similar affinity for Kr nor Ar. From the results, a mechanism is proposed such that the strong Ag-Xe interaction contains both an underlying physical and electronic aspect related to the formation of Ag nanoclusters within the chabazite pore geometry that alters the chabazite surface state such that Xe is preferentially adsorbed.

Introduction

The noble gases Xe and Kr are found naturally in low concentrations in the atmosphere at 0.087 ppm and 1.099 ppm, respectively, while Ar is the third most abundant gas in the atmosphere at a concentration of 0.934%. These noble gases possess useful properties which make them attractive for both research and commercial use. Currently, a select few countries are responsible for the majority of global Xe and Kr production resulting in the market for these gases subject to high amounts of volatility and scarcity as a result of extenuating circumstances (e.g., societal conflicts or natural disasters). Xe in particular has been proposed as an anesthetic,[1-2] and all three noble gases are used in specialized types of lighting. In addition to these practical uses, the atmospheric detection of Xe is used for monitoring undeclared nuclear tests for the purpose of verification of the Comprehensive Nuclear Test Ban Treaty.[3-4] Adsobents such as MOFS are also being considered for collection of Kr from spent nuclear fuel.[5-8] However, finding an efficient and cost-effective method for the capture and separation of noble gases (especially Kr and Xe) from air has proven to be technologically challenging. Generally, the commercial separation of these gases from air involves a cryogenic distillation process that is both energy intensive and expensive. This fact has incentivized the search for alternative forms or means of separation of these noble gases from the environment.

It has been shown that silver-exchanged zeolites in particular have a strong affinity for Xe, and much work has been done to explain the mechanism behind this interaction.[9-13] Other alternative adsorbents – such as MOFs – have also been explored as possible conduits to promoting Xe adsorption for separation purposes,[14-19] however, their viability for use on a commercial scale has yet to be demonstrated for this purpose. Zeolites are particularly attractive due to their ubiquity, low cost, ease of manipulation, and robust nature being able to maintain a stable state in more extreme environments (e.g., radioactivity, humidity, high temperatures, etc.) compared to MOFs.

While the mechanism behind silver's role in promoting Xe adsorption is still a subject of some contention, its ability to promote and improve Xe adsorption on various media has been well established. However, its effect on Kr and Ar adsorption has not been as similarly rigorously studied. This investigation was put forward to explore the mechanism behind this phenomenon and observe possible similar interactions with other metal cations. Presented here is the effect Cu, Pd, and Ag functionalization of chabazite have on the adsorption efficiencies of the noble gases Xe, Kr, and Ar. Cu and Pd were chosen as competitors to the "silver standard" due to their proximity to Ag on the periodic table. Cu and Ag are both members of Group 11 on the periodic table and share similar electronic structures. Pd and Ag are both on Row 5 of the periodic table and are more closely physically related (as measured by their empirical and Van der Waals radii).

Methods

Cation Exchange Procedure

A Na chabazite (CHA) zeolite was selected as the main adsorbent in this study as it is cheap, naturally occurring, easy to manipulate, and has been shown to have some affinity for the gases of interest in this study.[10-11, 20-21] The chabazite used in this study is a synthetic Na-chabazite (type R9160) sourced from Honeywell and was procured in the form of small pellets (between 20-50 US Sieve size). The cation exchange process involved adding a 10 mg/mL salt solution of the cation of interest to a small mass of zeolite in a 20:1 ratio of solution to zeolite (i.e., 200 mL of solution to 10 g of zeolite). This was then mixed on a benchtop shaker for 24 hours at room temperature. The solutions used were prepared from initially solid forms of $Cu(NO_3)_2$, $PdCl_2$, and $AgNO_3$ which were subsequently dissolved in DI water to achieve a 10 mg/mL concentration of the salt in solution. The zeolite mixture was then rinsed in DI water, vacuum filtered, and dried in an oven overnight at 110°C.

SEM/EDS

Each sample underwent scanning electron microscopy (SEM) and energy dispersive X-ray spectroscopy (EDS) to determine composition of the zeolites, confirm the presence of the exchanged cation of interest for each sample, and to determine whether any observable clustering of the metals had occurred on the zeolite surface. This was accomplished using a Hitachi SU8230 SEM equipped with an X-Max 150 Silicon Drift Detector. SEM images were taken at 5 kV while the EDS analyses were carried out at 15 kV. The resulting EDS concentrations were normalized to 100% after subtraction of carbon due to the use of carbon tape in staging of the sample during analysis.

Inverse Gas Chromatography

Ultra-high purity (UHP) He (99.999%) (carrier gas), UHP Ar (99.999%), research grade Xe (99.999%), and research grade Kr (99.999%) were purchased from Nexair. A Perkin Elmer Clarus 500 Gas chromatograph (GC) with TCD (Thermal Conductivity Detector) was used to analyze measurements taken for each sample. The column used for these experiments was a U-Loop packed with ~2g of zeolite sample (CHA, Cu-CHA, Pd-CHA, or Ag-CHA, depending on the experiment). The samples were outgassed at a high temperature of 320°C over a span of 18 hours before each set of analyses were performed. UHP He was used as the carrier gas for the GC and TCD, flowing at about 10.8 mL/min. Flow rate was measured, recorded, and adjusted (if needed) before each set of analyses to ensure consistency. The injector port was kept at 175°C and the TCD was kept at 300°C.

The inverse GC analysis procedure is as follows: 40µL of the analysis gas of interest were injected into the column packed with the unmodified chabazite (CHA) in the U-Loop of the GC. This was done in triplicate for each temperature at 100, 125, 150, 175, 190, and 200°C. The column was outgassed between each temperature change for 75 minutes at 320°C. A longer outgassing of 320°C over a span of 18 hours was started 24 hours before each analysis was performed in order to drive off water vapor and any other impurities present. This process was repeated for the silver chabazite (Ag-CHA), palladium chabazite (Pd-CHA), and copper chabazite (Cu-CHA) samples at

100, 125, 150, 175, 190, and 200°C. Xe was always selected as the final gas to be analyzed after both Ar and Kr analyses had been fully completed for each sample.

Henry's Law Constants (K) for each sample and noble gas of interest were calculated following equation (1):

$$(1)\ K = \frac{V_R Q}{mRT}$$

In this equation, V_R is the net retention time of the gas of interest (Ar, Kr, or Xe) from air, Q is the mass flow rate of the gas during the analysis (mL/min), T is the column temperature (Kelvin), m is the mass of the zeolite (grams), and R is the gas constant. The enthalpy of adsorption (ΔH) was determined following the relationship shown in equation (2):

$$(2)\ \ln(K) = -\frac{\Delta H}{RT} + C$$

Here, C represents a constant containing entropy information. In a plot of ln(K) and -1/RT for the gas and sample of interest, ΔH can be determined by simply finding the slope of the resulting line.

BET and Noble Gas Isotherms

All N_2, Kr, and Xe isotherms were collected using an Anton Paar Quantachrome Autosorb iQ Gas Sorption Analyzer instrument. The control program and analysis software was the AsiQwin program, version 4.0. Prior to analysis, all samples were outgassed at 300°C for 300 minutes and were then tested for the presence of residual water by monitoring the sample for a pressure rise at 300°C (ΔP<21 mTorr). Surface area analysis was carried out using nitrogen adsorption-desorption isotherms at 77K. Surface area and pore volumes were calculated using the density functional theory (DFT) method. Xe and Kr adsorption-desorption isotherms were taken at 323.15K and were run in triplicate for each sample. Ar adsorption isotherms were not taken as the GC analyses showed it had little to no affinity for any of the samples analyzed.

Results and Discussion

The chabazite used here contains a Si/Al ratio of ~2.7 as measured through SEM/EDS. This ratio holds for all samples (exchanged and unexchanged). The results of the SEM/EDS analysis show that the chabazite samples integrated more Ag during the cation exchange procedure than Cu or Pd. This is likely due to the different valence state of Ag (1+) compared to Cu and Pd(both 2+). We speculate that a higher proportion of Ag exchanged into the Na-chabazite structure over Cu or Pd to satisfy charge balances. This is reflected both in the higher weight percent of Ag in the Ag-CHA compared to Cu and Pd in their respective samples and also in the Ag-CHA containing a higher molar ratio of Ag/Na compared to the Cu/Na and Pd/Na ratios in the Cu-CHA and Pd-CHA samples, respectively (**Table 1**). Ag-CHA also exhibited both higher Ag/Ca and Ag/K molar ratios compared to Cu and Pd in their respective exchanged samples (**Table 1**).

	Cu-CHA (M=Cu)	Pd-CHA (M=Pd)	Ag-CHA (M=Ag)
M/Na	0.50	0.56	0.75
M/Ca	5.56	5.86	11.46
M/K	9.95	10.76	30.54
M (wt.%)	4.49±0.13	8.61±2.32	11.29±2.13

Table 1: Metal cation (M) molar ratios and weight percent as measured by SEM/EDS for the exchanged chabazite samples

However, despite this higher concentration of Ag in the Ag-CHA samples, the formation of Ag-microparticles on the surface of the zeolite itself was not observed, nor were there any Cu or Pd microparticles observed on either the Cu-CHA or the Pd-CHA samples. A previous study of a Ag-exchanged zeolite conducted by Deliere et al. shows that nanoparticle formation of approximately 3 nm occurred during the cation exchange procedure (which included a final reduction step not employed in this study).[9] Nanoparticles of this size are below the resolution achieved during the SEM analysis for this study, therefore, we cannot definitively dismiss the possibility of nanometer scale particle formation within the pores or along the surface of the chabazite samples prepared. A previous study by Coopersmith et al. also shows that reduction of Ag cations to metallic Ag resulted in particle formation on a chabazite surface, but particle formation was not observed in the unreduced samples. [22]

The surface area analysis results are displayed in **Table 2** and in **Figure 1**. The Cu-CHA surface area is nearly indistinguishable from that of the unexchanged chabazite sample (CHA) while the Pd- and Ag-CHA samples both display a lower total surface area. Ag-CHA is measured to have the lowest surface area and the lowest pore volume as calculated by DFT analysis by a significant margin. The lower pore volume and surface area exhibited by Ag-CHA combined with the higher exchange rate of Ag compared to the other metal cations and the lack of observable Ag clustering on the surface of the Ag-CHA by SEM (**Figure S1**) suggests that there is a higher amount of Ag captured within the pores

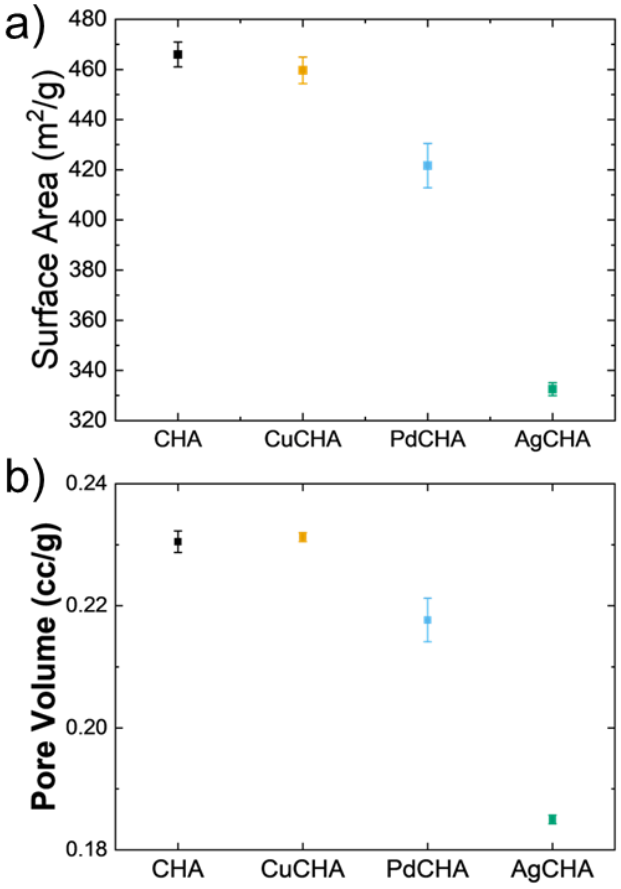

Figure 1: a) Surface area of the different chabazite samples as determined by DFT calculations from the ASiQwin program. b) Pore volume of the zeolites calculated in the same method.

of the Ag-CHA, possibly manifesting as Ag-nanoclusters akin to models proposed by Nguyen et al.[10]

Sample	DFT Surface Area (m^2/g)	Error (m^2/g)	DFT Pore Volume (cc/g)	Error (cc/g)
CHA	466	4	0.231	0.002
Cu-CHA	460	5	0.231	0.001
Pd-CHA	422	7	0.218	0.004
Ag-CHA	333	2	0.185	0.001

Table 2: Surface area and pore volume as calculated by DFT for all samples analyzed. Uncertainty is reported as standard error between analyses.

Xe and Kr adsorption isotherms for each sample are presented in **Figure 2a** and **b,** respectively. In all cases, the isotherms can be classified as the reversible Type I adsorption isotherm as described by Sing et al[23]. This indicates that the adsorbate of interest in these analyses reached a limiting capacity, and the adsorbate-adsorbent interactions observed are being governed by the available micropore volume as opposed to the total internal surface area. As seen in **Figure 2a**, the higher adsorbed volume of Xe on Ag-CHA at low partial pressures indicates that Xe is being preferentially adsorbed on strong sites specific to Ag-CHA not seen in the other samples analyzed here. The presence of strong adsorption sites is similar to what is reported by Daniel et al.[13] in other Ag-loaded zeolites. The formation of nanoparticles on the surface of the Ag-CHA for this study, however, was not observed as was previously noted. Interestingly, the capacity of Xe adsorbed on the Ag-CHA is lower than that of CHA and Cu-CHA suggesting that while those strong sites more readily accept Xe at lower partial pressures, the lower pore volume exhibited by Ag-CHA may be affecting its overall capacity to adsorb Xe to the extent exhibited by an

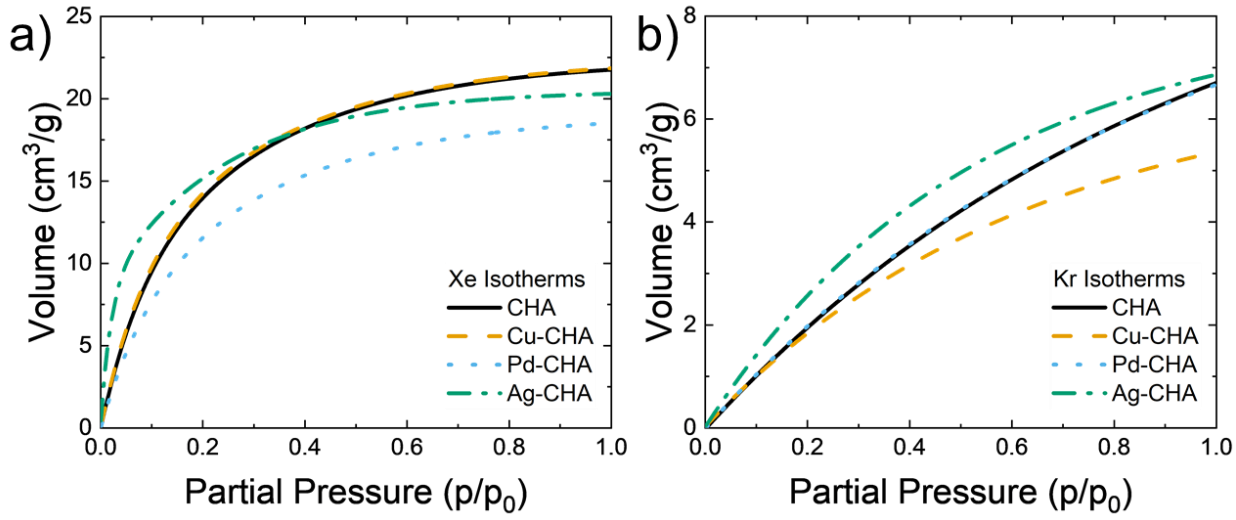

Figure 2: Adsorption isotherms for a) Xenon and b) Krypton for the different chabazite samples. Note the high uptake at low partial pressures for Ag-CHA in the Xe isotherm, indicative of strong binding sites within the metal exchanged zeolite.

unmodified chabazite.

The results of the inverse GC analyses are displayed in **Figure 3**. Retention times of Ar, Kr, and Xe were measured during the inverse GC analysis at temperatures ranging from 100 to 200°C. There was no observable difference in the retention times of Ar between the different samples, so those results are not included in **Figure 3** but can be viewed in the Supplemental Information (**Figure S2**). Values of ΔH as calculated following equation (2) are shown in **Table 3**. Plots of Henry's Law Constants calculated using equation (1) for the different gases at each temperature are shown in **Figure 4**. While there appears to be only slight differences between each samples' Henry's Law Constants for Ar and Kr, those calculated for Xe are much higher for Ag-CHA. When taken into account with the higher enthalpy of adsorption (**Table 3)** and longer retention time of Xe for Ag-CHA (**Figure 3**), the higher Henry's Law constants calculated for Xe likely relate to a change in the affinity of those sites for Xe as a direct result of the unique properties exhibited by Ag-CHA. This further illustrates Ag-CHA's affinity for Xe over the other samples analyzed.

	ΔH (kJ/mol)			
Gas of Interest	CHA	Cu-CHA	Pd-CHA	Ag-Cha
Ar	8.665 ± 0.154	9.747 ± 0.081	5.216 ± 0.094	7.468 ± 0.123
Kr	18.328 ± 0.031	18.434 ± 0.055	13.491 ± 0.011	16.699 ± 0.035
Xe	28.616 ± 0.061	29.823 ± 0.021	24.838 ± 0.011	39.079± 0.055

Table 3: Enthalpies of adsorption as calculated following Equation (2)

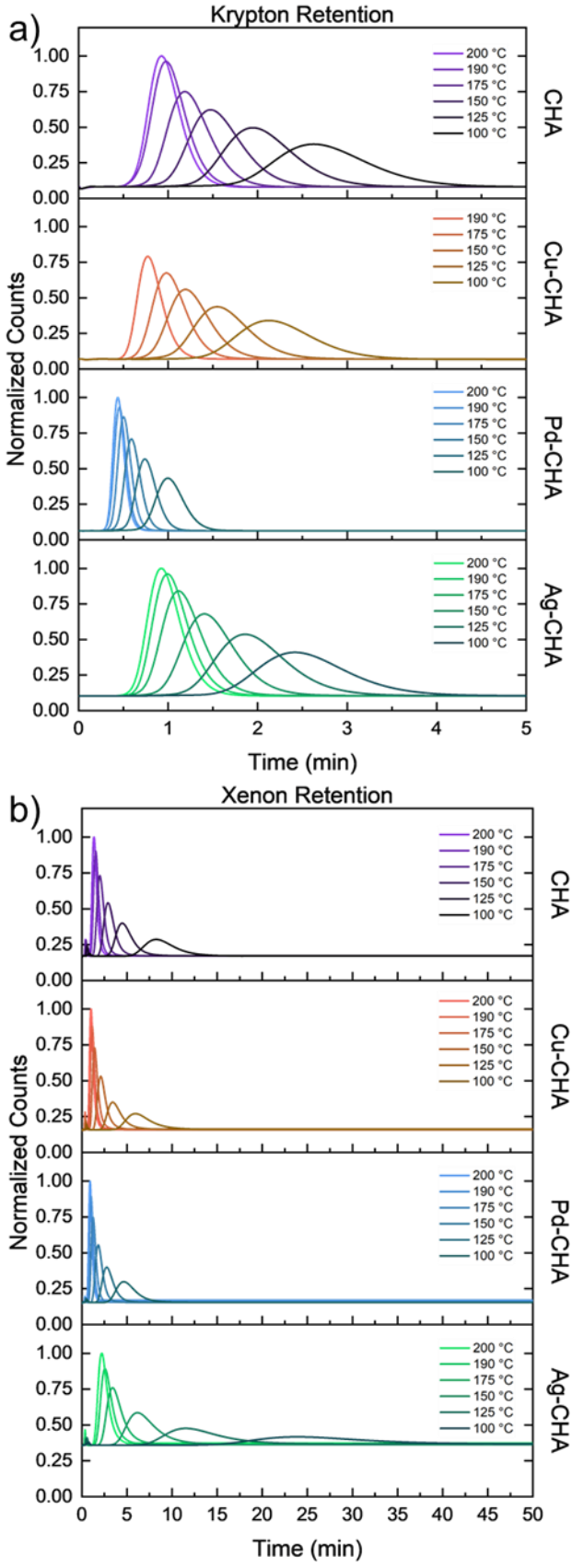

Figure 3: Inverse GC results for a) krypton and b) xenon retention in chabazite samples. All peaks for a given gas/metal zeolite are normalized to the maximum peak value of that series.

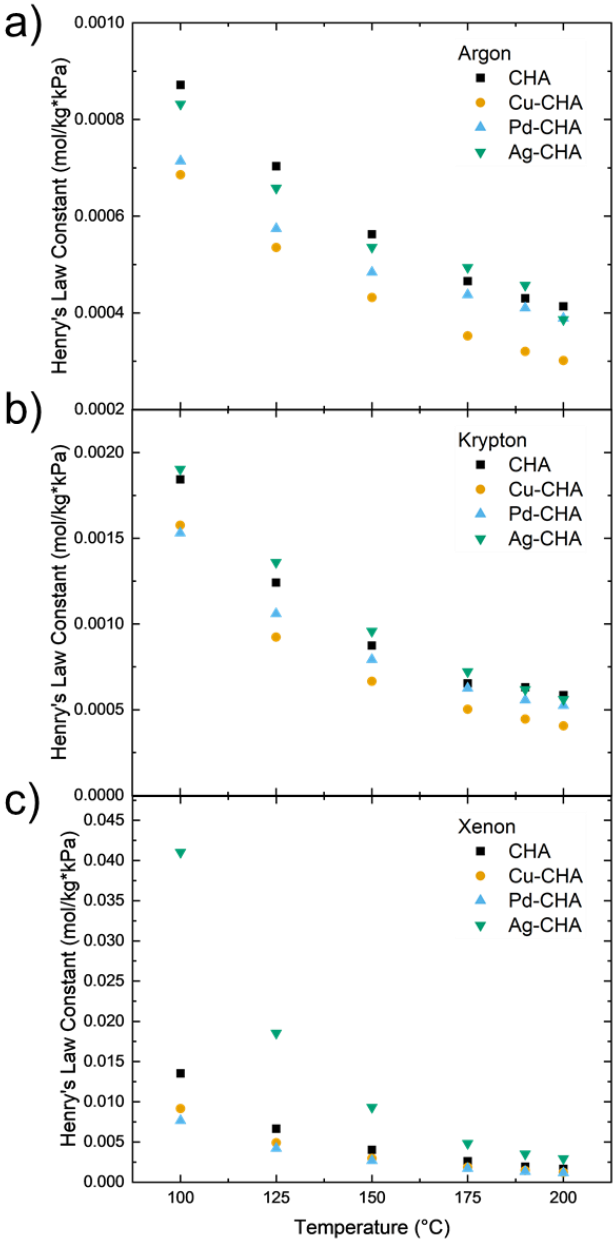

Figure 4: Henry's Law constants for a) argon, b) krypton, and c) xenon for the different chabazites.

Pd-CHA exhibited the lowest retention times for all gases at all temperatures out of the samples analyzed here. Calculations of ΔH (**Table 3**) for Pd-CHA also show it to have a lower affinity for the gases analyzed compared to the other samples, and it exhibits the lowest Xe/Kr selectivity (**Figure 5**). When taken in conjunction with the lower surface area and pore volume measured for Pd-CHA, this suggests that the lower pore availability exhibited by Pd-CHA compared to CHA and Cu-CHA is inhibiting its ability to adsorb these gases onto the zeolite surface. Since the adsorption isotherms suggest that availability of micropore volume is driving the interaction between Xe and the chabazite samples, this indicates that the lower available pore volume would be a cause for Pd-CHA's lower affinity for Xe (as well as Kr and Ar). While Ag-CHA also exhibits

a lower surface area and pore volume, the different electronic structure of Ag versus Pd must be an influence on the former's high affinity of the Ag-CHA for Xe.

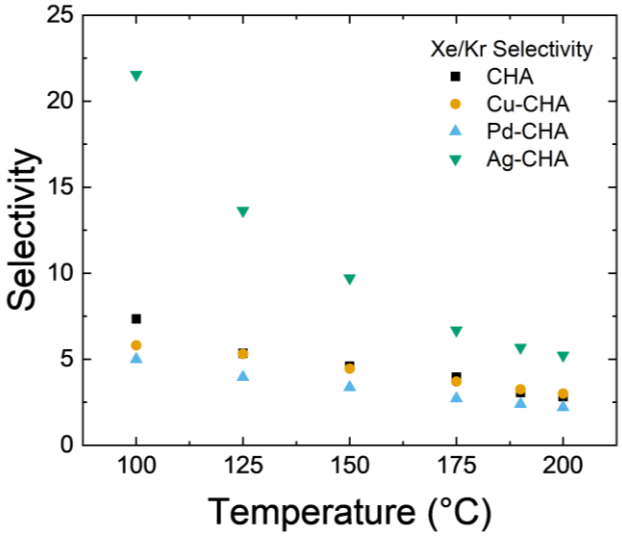

Figure 5: Xe/Kr selectivity of the different exchanged chabazites, assuming a 50/50 mixture of Kr/Xe.

While there was no observable formation of nanoparticles on the zeolite surface (**Figure S1**), the lower surface area and pore volume measured on the Ag-CHA, coupled with the higher exchange of Ag in the chabazite as evidenced by the SEM/EDS data, suggest that the Ag-CHA contains a higher amount of Ag within the pores of the chabazite compared to the other functionalized chabazites and their respective exchanged metals. This is interpreted that the Ag-CHA prepared contains small nanoclusters of Ag within the pores of the chabazite structure. Formation of silver nanoclusters on zeolite surfaces is not a new phenomenon and has been previously documented.[9, 12, 21, 24] In the context of the samples analyzed here, this appears to be a feature unique to the Ag-CHA not found in the other metal functionalized samples. The Cu-CHA and Pd-CHA both have similar metal molar ratios (**Table 1**), but the Pd-CHA displays a significantly lower surface area and pore volume than either the Cu-CHA or CHA. Since Pd is physically larger than Cu, it is proposed that the Pd is blocking more of the available pore volume in the chabazite structure compared to Cu. The Cu exchange within the chabazite appears to have had very little effect on the available pore volume. If the adsorption of Xe onto the chabazite surface was purely a physical interaction controlled by the pore availability, then Pd-CHA would exhibit a lower capacity and affinity for Xe than CHA or Cu-CHA, which it does. Ag-CHA, however, breaks this trend by having both the lowest pore volume and the highest affinity for Xe out of the samples included here, indicating that there is an electronic control to Xe affinity. However, if the interaction was purely an electronic one, then it would be expected for Cu-CHA to exhibit some marked increase in Xe affinity over CHA similar to Ag-CHA due to both Cu and Ag sharing a more similar electronic structure. This interaction was not observed here despite Cu and Ag both having similar electronic configurations suggesting that it is not a purely electronic interaction that is controlling the Xe affinity exhibited by Ag.

Taking both forms of evidence into account leads to the conclusion that there is both a physical and electronic component unique to the Ag-CHA system controlling its affinity for Xe. A combination of both a chemical and physical control on noble gas binding to metal cation clusters

is expressly modeled in Monpezat et al. as well.[25]From the evidence gathered here, it is not clear whether the Ag-CHA system could reach a limiting capacity for Xe affinity as a function of higher Ag functionalization, as only one concentration of functionalized Ag-CHA was prepared. It is possible that a fully exchanged Ag-CHA may prove less efficient or have a lower capacity to adsorb Xe if the higher exchange results in significant pore blockage. Alternatively, a higher exchange of Ag in the chabazite than that exhibited here could increase the Xe uptake as demonstrated by Daniel et al., if Xe affinity is dependent on the number of strong sites related to silver cluster formation.[13] Further work must be done to determine which hypothesis proves more accurate.

Krypton and Argon

While there was a marked difference between Xe retention times among the chabazite samples, the same cannot be definitively said for Ar or Kr. There appear some small differences between the retention times of Kr and Ar for all the samples as shown in **Figure 3** and **Figure S2**. Pd-CHA exhibits the lowest retention time for Ar and Kr followed by Cu-CHA and then Ag-CHA. All three metal-exchanged chabazite samples' Ar and Kr retention times were negatively affected by the cation exchange process when compared to the base CHA sample. The enthalpies of adsorption for Kr are higher than those calculated for Ar, but lower than those of Xe. Between the different samples, Cu-CHA and CHA have similar heats of adsorption with Ag-CHA having slightly lower ΔH and Pd-CHA having the lowest. The Kr adsorption isotherms show that all samples have an overall lower capacity for Kr than for Xe indicating that base CHA's pore structure itself is more agreeable to Xe adsorption than it is for Kr (or Ar). This is likely due to the different kinetic radii of the different noble gases in relation to the pore sizes in the chabazite. While Ag-CHA exhibits a higher uptake of Kr at most equivalent partial pressures (**Figure 2b**), the capacity of Kr is unchanged from that of either the CHA or Pd-CHA samples. Both Kr and Ar are also calculated to have lower heats of adsorption and Henry's Law Constants for these samples compared to those calculated for Xe.

From all of the evidence provided thus far, there is evidence that Ag nanoclusters within the pores of the Ag-CHA are important to Xe capture. Computational modeling of Ag cluster formation in Ag-functionalized chabazite has shown that small 3-8 atom clusters of Ag can form within the pores of the chabazite whilepotentially still being able to accommodate Xe uptake (L. Roy, *personal communication*). As such, it would be prudent to discuss an interpretation that would explain the differences observed between the noble gases and the metal exchanged chabazites.

For the noble gases, the van der Waals radii are slightly different, with Ar having a radius of 1.94 Å, Kr of 2.07 Å, and Xe of 2.28 Å.[26] The pore dimensions for the unexchanged chabazite were found by crystal structure measurements to be ~3.80 x 3.80 Å.[27] It is conceivable that Xe atoms just barely fit into the pores, but in doing so lose most of their thermal kinetic energy. The Xe atoms would then be in the pore of the chabazite with minimal thermal kinetic energy, as evident by larger Xe adsorption isotherm values across all chabazite samples. Kr, and even more so for Ar, would lose less kinetic energy when entering the pores due to its smaller size. These gases would then be more prone to being rebounded back outside of the chabazite pore structure. Once the chabazite samples are fully saturated by either Kr or Ar, there is a greater probability for these

gas atoms to leave the pores of the chabazite due to their smaller size from thermal kinetic motion. Xe however would be inhibited by its larger size.

The preference for Xe capture in Ag exchanged chabazites, however, is not wholly a physical one. As mentioned previously, there are indications of charged cluster formation within the pores of Ag-exchanged chabazite samples based on the change in pore volume as seen in **Table 2.** Pd atoms are of a comparable size to that of Ag atoms. However, the Pd samples have a worse retention and uptake of all the noble gases indicating the blocking of pores by Pd atoms. The silver clusters and cations must have another interaction with Xe which is inferred to be electronic in nature. Cu-CHA almost exactly aligns with the CHA samples in the Xe adsorption isotherm. Since Cu has a similar electronic structure to Ag, it is reasonable to assume that it is some electronic interaction unique to Ag cations or Ag clusters. It has been proposed in previous work that either σ donation between Xe and ionic clusters of Ag or d_π-d_π back-donation are the dominant role in this Xe-Ag interaction.[10, 28] With the observation of strong sites in the Xe adsorption isotherm,[13] the presented experimental evidence indicate that this might be a silver cluster electronic interaction that differs from the interaction with the Ag cation which supports the model proposed by Nguyen et al.[10]

Combining both these inferences, one could then see why there is such an increased retention and selectivity for Xe in Ag exchanged chabazites from both a physical and electronic interaction. The Xe atoms would lose most of their thermal kinetic energy when entering the chabazite pore with Ag clusters and cations present. Once contained in the pores, and with unfavorable conditions to leave the chabazite structure, the Ag clusters and cations would then exert an electronic interaction to further confine the Xe atoms within the chabazite pore structure. It would then be unlikely for the Xe to exit outside the Ag exchange chabazite, as seen by the trend in retention time (**Figure 3**) and increase in Henry's Law Constant at lower temperature (**Figure 4**). Additional Xe atoms could then interact with the same Xe-filled pore and push the Xe further into the chabazite structure, like the mechanisms proposed for MOFs' noble gas capture.[18] Other gases would not have this dual mechanism for capture experienced by Xe and would thus have diminished retention within the Ag exchanged chabazites.

Conclusions

The noble gases Xe, Kr, and Ar possess many desirable properties that make them important in both the commercial and research spheres. In addition to their economic importance, monitoring of Xe is key to validating international compliance with the Comprehensive Nuclear Test Ban Treaty. The current process of separating Xe and Kr from air is expensive, energy intensive, and localized within a few select countries. Therefore, the exploration of alternative materials with high affinities for these gases presents an excellent opportunity to mitigate many of these problems. Ag-functionalized materials have previously demonstrated such affinities for Xe, but the mechanism behind this relationship is still debated in the present literature. Here we have directly measured the affinity of the noble gases Xe, Kr, and Ar for multiple metal-exchanged (Cu, Pd, Ag) forms of Na-chabazite. We have shown that the relationship that drives affinity is derived from both a favorable electronic interaction between the surface and the gas of interest coupled with a specific physical component related to surface pore availability and structure. For efficient adsorption for the purpose of separation of these noble gases, both the physical and electronic

aspects of the material of interest must be accounted for in the pursuit of an ideal noble gas adsorbent.

Through the preparation of various metal exchanged forms of chabazite, the following was demonstrated:

1. Ag functionalized chabazite has a higher affinity for Xe than CHA, Pd-CHA, and Cu-CHA with an enthalpy of adsorption of 39.1 kJ/mol. Despite this affinity for Xe, a similar interaction is not observed for Kr and Ar.
2. The higher exchange of Ag in the chabazite structure resulted in a lower available pore volume and surface area which can be explained by the formation of small (likely 3-8 atom) Ag nanoclusters within the chabazite pores.
3. Strong sites within the Ag-CHA have a higher affinity for Xe at low partial pressures than CHA, Pd-CHA, and Cu-CHA, but Ag-CHA has a lower overall capacity for Xe than CHA and Cu-CHA. This is likely a result of Ag-CHA's lower pore volume availability.
4. The low pore volume and surface area exhibited by Pd-CHA is a result of pore blockage or other form of interference by the Pd on the chabazite surface. While it is more physically similar to Ag than Cu, Pd's different electronic configuration indicate that there is an electronic control relating Ag's affinity for Xe.
5. Despite Cu and Ag's similar electronic configuration, Cu-CHA did not exhibit the same affinity for Xe as Ag-CHA. Cu-CHA and CHA's near identical pore volume and surface area coupled with both samples' near indistinguishable affinity for Xe indicate that there is likely an additional physical component to the affinity for Xe exhibited by Ag-CHA.
6. The formation of Ag nanoclusters within the pores of the Ag-CHA lead to both a physical and electronic change in the surface state of the chabazite that promote its affinity for Xe.

Supporting Information

SEM images of cation exchanged chabazite surfaces, additional inverse GC retention plot for Argon

Acknowledgements

All authors listed contributed equally to this study and preparation of this manuscript. Funding for this work was supported by the Defense Threat Reduction Agency (DTRA) under Interagency Agreement number DTRA13081-38811. This work was produced by Battelle Savannah River Alliance, LLC under Contract No. 89303321CEM000080 and a predecessor contract with the US Department of Energy. Publisher acknowledges the U.S. Government license to provide public access under the DOE Public Access Plan (http://energy.gov/downloads/doe-public-access-plan).

References

1. Cullen, S. C.; Gross, E. G., The Anesthetic Properties of Xenon in Animals and Human Beings, with Additional Observations on Krypton. *Science* **1951**, *113*, 580-582.
2. Lynch, C.; Baum, J.; Tenbrinck, R.; Weiskopf, Richard B., Xenon Anesthesia. *Anesthesiology* **2000**, *92*, 865-870.

3. Ross, O.; Ahlswede, J.; Annewandter, R.; Kalinowski, M. B.; Rast, S.; Schluenzen, K. H. *Simulations of Atmospheric Krypton-85 to Assess the Detectability of Clandestine Nuclear Reprocessing*; International Atomic Energy Agency (IAEA), 2010; p 8.
4. Fontaine, J. P.; Pointurier, F.; Blanchard, X.; Taffary, T., Atmospheric Xenon Radioactive Isotope Monitoring. *Journal of Environmental Radioactivity* **2004**, *72*, 129-135.
5. Elsaidi, S. K.; Mohamed, M. H.; Helal, A. S.; Galanek, M.; Pham, T.; Suepaul, S.; Space, B.; Hopkinson, D.; Thallapally, P. K.; Li, J., Radiation-Resistant Metal-Organic Framework Enables Efficient Separation of Krypton Fission Gas from Spent Nuclear Fuel. *Nature Communications* **2020**, *11*, 3103.
6. Greenhalgh, M. R.; Garn, T. G.; Welty, A. K.; Lyon, K. L.; Watson, T. L. *Multi-Column Experimental Test Bed for Xe/Kr Separation*; Idaho National Lab.(INL), Idaho Falls, ID (United States): 2015.
7. Thallapally, P. K.; Robinson, A. J.; Zbib, A. A.; Riley, B. J.; Chong, S.; Liu, J.; Murphy, M. K.; Okabe, P.; Sherrod, R. *Noble Gas Management: Sbmof 1 Vs. Nucon Carbon*; Pacific Northwest National Lab.(PNNL), Richland, WA (United States): 2022.
8. Welty, A. K.; Greenhalgh, M. R.; Garn, T. G. *Multi-Column Experimental Test Bed Using Casdb Mof for Xe/Kr Separation*; Idaho National Lab.(INL), Idaho Falls, ID (United States): 2016.
9. Deliere, L.; Topin, S.; Coasne, B.; Fontaine, J.-P.; De Vito, S.; Den Auwer, C.; Solari, P. L.; Daniel, C.; Schuurman, Y.; Farrusseng, D., Role of Silver Nanoparticles in Enhanced Xenon Adsorption Using Silver-Loaded Zeolites. *The Journal of Physical Chemistry C* **2014**, *118*, 25032-25040.
10. Nguyen, H. G.; Konya, G.; Eyring, E. M.; Hunter, D. B.; Truong, T. N., Theoretical Study on the Interaction between Xenon and Positively Charged Silver Clusters in Gas Phase and on the (001) Chabazite Surface. *J Phys Chem C* **2009**, *113*, 12818-12825.
11. Saxton, C. G.; Kruth, A.; Castro, M.; Wright, P. A.; Howe, R. F., Xenon Adsorption in Synthetic Chabazite Zeolites. *Microporous and Mesoporous Materials* **2010**, *129*, 68-73.
12. Kuznicki, S. M.; Anson, A.; Koenig, A.; Kuznicki, T. M.; Haastrup, T.; Eyring, E. M.; Hunter, D., Xenon Adsorption on Modified Ets-10. *J Phys Chem C* **2007**, *111*, 1560-1562.
13. Daniel, C., et al., Xenon Capture on Silver-Loaded Zeolites: Characterization of Very Strong Adsorption Sites. *The Journal of Physical Chemistry C* **2013**, *117*, 15122-15129.
14. Banerjee, D.; Cairns, A. J.; Liu, J.; Motkuri, R. K.; Nune, S. K.; Fernandez, C. A.; Krishna, R.; Strachan, D. M.; Thallapally, P. K., Potential of Metal–Organic Frameworks for Separation of Xenon and Krypton. *Accounts Chem Res* **2015**, *48*, 211-219.
15. Banerjee, D.; Simon, C. M.; Elsaidi, S. K.; Haranczyk, M.; Thallapally, P. K., Xenon Gas Separation and Storage Using Metal-Organic Frameworks. *Chem* **2018**, *4*, 466-494.
16. Elsaidi, S.; Ongari, D.; Mohamed, M.; Xu, W.; Motkuri, R.; Haranczyk, M.; Thallapally, P., Metal Organic Frameworks for Xenon Storage Applications. *ACS Materials Letters* **2020**, *2*, 233-238.
17. Li, J. L.; Huang, L.; Zou, X. Q.; Zheng, A. M.; Li, H. Y.; Rong, H. Z.; Zhu, G. S., Porous Organic Materials with Ultra-Small Pores and Sulfonic Functionality for Xenon Capture with Exceptional Selectivity. *J Mater Chem A* **2018**, *6*, 11163-11168.
18. Li, L.; Guo, L.; Zhang, Z.; Yang, Q.; Yang, Y.; Bao, Z.; Ren, Q.; Li, J., A Robust Squarate-Based Metal–Organic Framework Demonstrates Record-High Affinity and Selectivity for Xenon over Krypton. *Journal of the American Chemical Society* **2019**, *141*, 9358-9364.
19. Xiong, X.-l.; Chen, G.-h.; Xiao, S.-t.; Ouyang, Y.-g.; Li, H.-b.; Wang, Q., New Discovery of Metal–Organic Framework Utsa-280: Ultrahigh Adsorption Selectivity of Krypton over Xenon. *The Journal of Physical Chemistry C* **2020**, *124*, 14603-14612.
20. Feng, X.; Zong, Z.; Elsaidi, S. K.; Jasinski, J. B.; Krishna, R.; Thallapally, P. K.; Carreon, M. A., Kr/Xe Separation over a Chabazite Zeolite Membrane. *Journal of the American Chemical Society* **2016**, *138*, 9791-9794.
21. Liu, Y.; Chen, F.; Kuznicki, S.; Wasylishen, R.; Xu, Z., A Novel Method to Control the Size of Silver Nanoparticles Formed on Chabazite. *Journal of nanoscience and nanotechnology* **2009**, *9*, 2768-71.

22. Coopersmith, K. J.; Broadwater, K. L.; Demers, S. M. E.; Monikandan, R.; Torcivia, M.; Roy, L.; Hunter, D., Investigating the Role of Silver Oxidation State on the Thermodynamic Interactions between Xenon and Silver-Functionalized Zeolites. *The Journal of Physical Chemistry C* **2023**.
23. Sing, K. S. W., Reporting Physisorption Data for Gas/Solid Systems with Special Reference to the Determination of Surface Area and Porosity (Recommendations 1984). *Pure Appl Chem* **1985**, *57*, 603-619.
24. Deliere, L.; Coasne, B.; Topin, S.; Gréau, C.; Moulin, C.; Farrusseng, D., Breakthrough in Xenon Capture and Purification Using Adsorbent-Supported Silver Nanoparticles. *Chemistry (Weinheim an der Bergstrasse, Germany)* **2016**, *22*, 9660-6.
25. Monpezat, A.; Aupiais, J.; Siberchicot, B., Xe Adsorption on Noble Metal Clusters: A Density Functional Theory Investigation. *ACS Omega* **2021**, *6*, 31513-31519.
26. Vogt, J.; Alvarez, S., Van Der Waals Radii of Noble Gases. *Inorganic Chemistry* **2014**, *53*, 9260-9266.
27. Yue, Q.; Halamek, J.; Rainer, D. N.; Zhang, J.; Bulánek, R.; Morris, R. E.; Čejka, J.; Opanasenko, M., Tuning the Cha Framework Composition by Isomorphous Substitution for Co2/Ch4 Separation. *Chemical Engineering Journal* **2022**, *429*, 131277.
28. Grosse, R.; Burmeister, R.; Boddenberg, B.; Gedeon, A.; Fraissard, J., Xenon-129 Nmr of Silver-Exchanged X-and Y-Type Zeolites. *The Journal of Physical Chemistry* **1991**, *95*, 2443-2447.